The determination of the lower critical concentration temperature and intrinsic viscosity: The syneresis reaction of polymeric gels

Ako, K., Elmarhoum, S. & Munialo, C. D

Original citation & hyperlink:
Ako, K, Elmarhoum, S & Munialo, CD 2022, 'The determination of the lower critical concentration temperature and intrinsic viscosity: The syneresis reaction of polymeric gels', Food Hydrocolloids, vol. 124, no. Part B, 107346.
https://doi.org/10.1016/j.foodhyd.2021.107346

DOI 10.1016/j.foodhyd.2021.107346
ISSN 0268-005X
ESSN 1873-7137

Publisher: Elsevier

The determination of the lower critical concentration temperature and intrinsic viscosity: the syneresis reaction of polymeric gels

Authors and affiliations:

Komla AKO * [a], Said ELMARHOUM [a], Claire D. MUNIALO [b]

a) Univ. Grenoble Alpes, CNRS, Grenoble INP*, LRP, 38000 Grenoble, France

b) School of Life Sciences, Coventry University, Priory Street, Coventry, CV1 5FB, UK

***Corresponding author**: *komla.ako@univ-grenoble-alpes.fr*; *akokomla@hotmail.com*

Abstract

This work studies (by rheological method) the temperature dependence of coil-to-coil contact critical concentration (C* in g/L) and the intrinsic viscosity ([η] in L/g) as the capacity of a single-coil to bind the solvent molecules and increase the solution viscosity accordingly. The C* and [η] were measured and fitted by a model to characterize the thermodynamic stability of the kappa-carrageenan (kC) polysaccharide in solution. The weakest C* and greatest [η] of the kC was found to be ≈ 0.44 g/L and ≈ 1.23 L/g, respectively. The temperature where the C* was weakest was found at ≈ 30 °C and is referred to as the lower critical concentration temperature (LCCT). The expansion of the polysaccharide was greater at the LCCT, but its capacity to bind the solvent molecules was found greater at 20 °C according to the model. The hydrodynamic permeability resistance was defined as C*[η] and was shown to decrease smoothly by a slope of 2.6×10^{-3} /°C with the increase in temperature from 0 °C to 45 °C, then strongly by a slope of 22.5×10^{-3} /°C after 60 °C. Therefore, if a polymer solution at LCCT is gelled at lower or higher temperature, the polymer sizes will decrease (syneresis reaction), but the [η] and gel elasticity

will interfere with the kinetics of the reaction to determine thereafter the serum holding capacity of the gels.

Keywords: Rheology, polymers expansion, hydrodynamic volume, water-holding capacity

1. Introduction

Kappa-Carrageenan (kC) is a polysaccharide that is extracted from marine algae, which forms gels in the appropriate conditions such as polysaccharide concentration, ionic strength, type of ions, and temperature (Ciancia, Milas & Rinaudo, 1997; Morris & Chilvers, 1983). However, the gels that are formed by kC in the presence of K^+ and Ca^{2+} ions have been characterized by the spontaneous release of water (syneresis) (Lai, Wong & Lii, 2000). The elasticity is reported to explain the syneresis of these gels (Ako, 2015; Mao, Tang & Swanson, 2001). Other polysaccharide gels such as starch, alginate, agar and pectin have also been reported to be susceptible to syneresis (Divoux, Mao & Snabre, 2015; Draget et al., 2001; Einhorn-Stoll, 2018; Lee, Baek, Cha, Park & Lim, 2002).

As a natural resource, polysaccharides form the major component of the human diet and are therefore used by the food industries to process food with particular specifications (Kaur, Singh & Sodhi, 2002; Lee, Baek, Cha, Park & Lim, 2002; Teko, Osseyi, Munialo & Ako, 2021). For instance, polysaccharides are used as thickeners and viscosity controlling agents of many suspensions and beverages for managing swallowing disorders for dysphagic patients and the elderly (Munialo, Kontogiorgos, Euston & Nyambayo, 2020; Yousefi & Ako, 2020). In most cases, foods that are made with thickeners and viscosity controlling agents are usually stored until consumption, which in some cases may be more than 3 months. However, a prolonged storage of polysaccharide suspensions which are susceptible to syneresis promotes the exhibition of the syneresis (Mao, Tang & Swanson, 2001). The duration that it takes for these

systems to exhibit syneresis is not yet well understood even though the chemical nature and associative mechanism of the constituents have been reported (Boral, Saxena & Bohidar, 2010; Scherer, 1989). This time depends on the chemical or mechanical kinetics of the ageing or phase separation which induces the syneresis process (Scherer, 1989; Takeshita, Kanaya, Nishida & Kaji, 2001; Vliet, Dijk, Zoon & Walstra, 1991), and the technique or method used for the detection of the polysaccharide susceptibility to syneresis (Ako, 2015; Einhorn-Stoll, 2018; Richardson & Goycoolea, 1994). When syneresis is discovered accidentally after several weeks of storage, it may cause considerable waste of time, matter, energy and money for the companies. Kappa-carrageenan and those polysaccharides that are susceptible to syneresis have many applications in pharmaceutical and biomedical industries, including cosmetic surgery, surface coating for drug and protein carriers, making them ubiquitous in our daily life (Berger, Reist, Mayer, Felt & Gurny, 2004; Field & Kerstein, 1994; Hoffman, 2012; Klouda & Mikos, 2008; Liu, Subhash & Moore, 2011). Their capacity to form strong gels and biocompatibility extends the application areas to designing 3D structures as scaffolds or cell culture substrates for tissues engineering (Drury & Mooney, 2003). Therefore, the inadvertent occurrence of syneresis may be lethal for biomedical and pharmaceutical applications. The growth of cells in agar gels for the detection of diseases for instance is damaged by the syneresis phenomena as the solvent is released with the cell nutrients. Mechanical contact problems also arise from the instabilities of gel dimensions (Divoux, Mao & Snabre, 2015). Chemical and mechanical aspect of the syneresis converge to i) chemical modification (Campo, Kawano, da Silva Jr & Carvalho, 2009), ii) the use of super gelling agents, and iii) an increase of material concentration (Zhang, Ji, Liu & Feng, 2016) to stop the occurrence of syneresis. However, it is not yet clear whether these methods actually stop the syneresis or they simply delay the time it takes to exhibit syneresis.

Kappa-Carrageenan (kC) and in general polysaccharides are processed in solution at temperatures between 60 °C and 90 °C then the solutions or gels are cooled and stored at ambient or lower temperatures before applications (Ako, 2015; Mao, Tang & Swanson, 2001). Given the temperature changes that occur from the sample preparation to their applications, the thermodynamic stability of the kC polysaccharide in solution at various temperatures were investigated in this study. In general, gels can reach the thermodynamic equilibrium very fast if their constituent units can move freely, i.e. no additional energy is required for the motions such as contraction, stretching, rotation or diffusion. Ideally, free contraction motion of the kC chains should take place conceptually at concentration below or equal to the critical concentration (Morris, Cutler, Ross-Murphy, Rees & Price, 1981) without energy of liaison at the contact points. The critical concentration C* is reciprocal to the volume of the smallest mass moving freely which is the blob stand by the polysaccharide chain. At C*, the concentration of the solution is equal to the concentration (of or defined by) a polymer chain volume in the solvent. The intrinsic viscosity [η] which is the capacity of the polysaccharide to increase the viscosity of the system has been determined by a linear Huggins and Kraemer analysis and used to characterize the interaction between the polymers and the solvent molecules (Brunchi, Morariu & Bercea, 2014; Chronakis, Doublier & Piculell, 2000). In this study, we define the [η] parameter as the capacity of a polymer chain to bind the solvent molecules and show that both physical quantities, C* and [η], are time-independent. The sensitivity of both quantities to the temperature is demonstrated to show the susceptibility of the polysaccharide to syneresis at the macromolecular scale. Supposing for instance that change of the temperature leads to remarkable change of the [η] and C*, then the system must evolve toward a new equilibrium state with a time evolution function that would depend on the stresses in competition in the systems.

In this work, the evolution of the C* as a function of the temperature was investigated using a model that allows the determination of the C* in the temperature interval from 0 °C to near 100 °C.

2. Materials and methods

2.1 Sample characteristics

The kappa-carrageenan (kC) polysaccharide was kindly provided by Rhodia Food (Switzerland), product name and reference: MEYPRO-GEL 01/2001 WG95-37 K-Car. The kC is made of a sequence of alternating disaccharides, α-(1-3)-D-Galactose-4-Sulfate and β-(1-4) -3,6-anhydrous-D-Galactose. The dialyzed product may contain a weak amount of glucose and was found in the pure potassium kC form of total potassium no more than 4.2 % (w/w), the other salts are considered to be only trace amounts. The molecular weight of the kC was M_w = 3.3×10^5 g/mol and the indices of polydispersity (Ip) = 2.02. It is worth mentioning that the kC is a polyelectrolyte and thermoreversible polymer. The kC in solution can turn from liquid to solid state by cooling and from the solid to liquid state by heating. This behaviour makes kC a perfect material for temperature ramp measurements to be repeated at different conditions on the same sample. During the cooling ramp, kC changes from random coil to helix conformation. The temperature where the coil-helix transition takes place is dependent on the ionic strength and the type of salt. The coil-helix transition takes place during heating ramp at temperature above the coil-helix transition temperature. The coil-helix transition changes the flow properties of the solution.

2.2 Sample preparation

Twenty g/L of kC solution was prepared by dissolving the powder in demineralized water in the presence of 200-ppm sodium azide (NaN_3) as a bacteriostatic agent. The mixture was then

heated at 90 °C under stirring for 10 h. The solution was then dialyzed in 4 L of ultrapure water in the presence of 200-ppm NaN_3 for 3 days using a dialysis membrane of 6-8 kDa molecular weight cut off. The dialysis water was exchanged thrice the first day and twice the second and third day respectively. The dialyzed solution was then filtered with Anotop syringe filter with 0.45 μm pore size to constitute the stock solution. The final concentration of the stock solution was adjusted by the dilution factor after the dialysis step. All samples that were analyzed were prepared by diluting the stock solution to give the desired final kC concentration and mixed under heating in a water bath at 60 °C for approximately 15 min to give homogeneous solutions prior the viscosity measurements. The system is comparable to a polyelectrolyte polymer solution with no additional salt except the presence of 200-ppm NaN_3, which was added to prevent spoilage of the samples.

2.3 Viscosity measurements

The viscosity measurements were performed in Couette geometry using a DHR3 Rheometer (TA Instrument). The Couette geometry consisted of a concentric cylinder geometry of an inner rotor cylinder (bob) and outer stator cylinder (cup) of respectively a radius R_1 of 14 mm and R_2 of 15 mm defining a horizontal gap (R_2 - R_1) of 1 mm and an average radius (R) of 14.5 mm as (R_1 + R_2)/2. The height of the bob was 42 mm and the vertical gap between the bob and cup was set at 2 mm. The minimum and maximum torque of the instrument were 5 μNm and 5×10^3 Nm respectively. Both the torque (M) and the angular velocity (Ω) of the bob were measured by the rheometer. The Ω is related to the shear rate by the expression:

$$\dot{\gamma} = \frac{R}{R_2 - R_1} \cdot \Omega \qquad (1)$$

and the shear stress is related to the torque by the expression:

$$\sigma = \frac{1}{2\pi h R^2} \cdot \mathrm{M} \tag{2}$$

Shear viscosity is defined as the shear stress divided by the shear rate, which is proportional to M/Ω, by the constant:

$$K_G = \frac{R_2 - R_1}{2\pi h R^3} \tag{3}$$

which is considered as the geometry constant applied by the DHR3 software (TA Instruments V9.49) to convert M/Ω into a viscosity data. The expression of the bob wall velocity is deduced as:

$$v_0 = \frac{R_1 \cdot (R_2 - R_1)}{R} \dot{\gamma} \tag{4}$$

When Eq.4 is compared with the velocity of plate-plate geometry wall of radius R_1 having the same Ω on a gap = R_2 - R_1, the comparison yields the following relationship of the shear rate between the plate-plate geometry and Couette geometry:

$$\dot{\gamma}_p = \frac{2R_1}{R_2 + R_1} \dot{\gamma} \approx 0.96\dot{\gamma} \tag{5}$$

This gives the factor between the viscosity from plate-plate geometry and Couette geometry. The results obtained by the use of a Couette geometry were comparable. However, it is worth to note that theoretically the Couette shear rate is higher than the plate shear rate by 4 %.

The temperature of the samples was controlled with a precision of ± 0.5 °C by a water circulation thermoregulator (Microcool LAUDA MC600). Prior to this study, the viscosity of the stock solution and a series of diluted samples were tested. The viscosity was determined as a function of the shear rate from 0.3 s^{-1} to 30 s^{-1} to define the Newtonian flow domain at a constant temperature in the range between 5 °C and 60 °C. The viscosity was also measured at

a constant shear rate of 15 s^{-1} while cooling or heating at 2 °C min^{-1} or a lower rate 0.5 °C min^{-1}. The viscosity was neither affected by the oil nor by the evaporation when 8 mL of the samples were introduced in the Couette and covered with 1 mL of mineral oil. Seven g/L stock solution was kept at 5 °C and the viscosity was measured over 2 months using the reported shear rate intervals. The viscosity of the stock solution was constant over the interval of shear rate and storage time. For all the samples tested in this study, the viscosity of a given concentration was shown to exclusively depend on the temperature and not on the shear rate except in cases where there was an experimental error. Therefore, all the samples of the study behave like Newtonian fluids, and their viscosity can be assimilated to the zero shear viscosity. The measurement of the viscosity including the viscosity of the solvent was done at 15 s^{-1} shear rate to yield a sensitive torque value.

2.4. Temperature dependence of the viscosity analysis

The viscosity of the solvent was measured as the solvent contributes to the viscosity of the sample. The viscosity of the solutions as a function of the concentration must cross the viscosity axis at the solvent viscosity. Although the viscosity of water is reported in literature, its value by the instrument used in this study is unknown because it may depend on the constant of the geometry (Eq.5) used to perform the measurement. Moreover, the viscosity of the solvent gives an insight on the precision of the instrument while measuring the viscosity of the sample at concentrations approaching zero. The raw data of the temperature dependence of the viscosity of the solvent (demineralized water with 200-ppm NaN_3) is shown in **Figure 1**. The values of the viscosity of water by DHR3 rheometer using Couette geometry and the value reported by Korson et al 1969 (Korson, Drost-Hansen & Millero, 1969) for water using Cannon- Ubbelohde viscometer are in good agreement by a constant factor. Therefore, the viscosity data analyses should not depend on this factor. The Couette geometry viscosity was greater than the Cannon-Ubbelohde viscosity by 10 %, which could be attributed to the geometry effects.

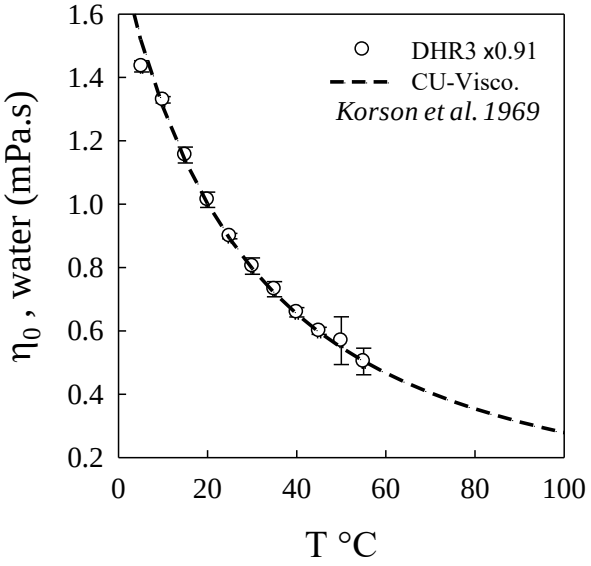

***Figure 1**: Temperature dependence of the viscosity of demineralized water in presence of 200-ppm of NaN_3. The viscosity by the DHR3 instrument using the Couette geometry and the viscosity reported by Korson et al. 1969 using Cannon-Ubbelohde viscometer (CU-Visco) are shown in Figure 1. The viscosity data by the DHR3 were multiplied by a factor of 0.91 to yield the same viscosity with the standard. The temperature values should be considered with ± 0.5 °C. The vertical viscosity error bars are ± the standard deviation of the viscosity from the corresponding temperature interval.*

The standard deviation of the viscosity increases with the temperature. This fact impedes the calculation of accurate specific viscosity $\eta_{sp} = (\eta-\eta_0)/\eta_0$. When the sample viscosity is close to the solvent viscosity, for temperatures > 50 °C and concentrations < 0.01 % (w/w) the fluctuation may yield negative η_{sp}.

The viscosity can be understood by the association of a perfect elastic (spring) and gas systems. Thus, we propose the following modelling of the temperature dependence of Newtonian fluid viscosity. The model is a concept based on the definition of the Newton's law of dynamic viscosity i.e. the rate of transfer of momentum across a unit area as the measurement of the resistance of a fluid to deformation at a given rate. The experimental viscosity is equivalent to

mass per unit of length and time, and this mass can be represented by a force if it is just scaled with the gravitational constant g ($F = m_{eq} \times g$). Given that the mass is the equivalence of the resistance of the fluid to deformation, this mass reflects the resistance to displacement of any single particle of the fluid. This mass is noted here as m_{eq} and is the expression of the sum of a "static" and "dynamic" mass. The static mass, m, is the mass of the fluid flowing without any interactions between the particles in motion. This mass is the conventional mass, and it does not depend on the temperature as it is conserved. The dynamic mass, m_D, is given here to represent the interaction forces between all the fluid constituents, which could also be referred to as the virial mass of the system. The dynamic mass is null, if the fluid is treated as a perfect gas. Given that the interaction forces between the solvent molecules depend on temperature, the m_{eq} as the viscosity depends on the temperature too.

$$m_{eq}^{T} = m_{D}^{T} + m \qquad 6$$

Hence, for a given system, the m_{eq} per unit of length and time evolves with the temperature following the temperature dependence of the m_D, which is related to the force at work in the system. At a given temperature, the model to give the m_{eq} uses the property of perfect spring and considers that the m_{eq} deforms a perfect spring on undetermined length (z) for a given time Δt or on a given length (z) but for an undetermined time. If the force is scaled with the restoring force constant k_o ($F = k_o \times z$), it results in the relation:

$$m_{eq}^{T} \cdot g = k_o \cdot z^{T} \qquad (7)$$

which equalizes the resistance of the fluid and the resistance of the spring (restoring force), with both resistances being dependent on temperature. The temperature dependence of z characterizes the influence of temperature on the interaction forces between the fluid constituents as m_D and the constituents' momentum as m. The flow could be pictured as the

stretching of a perfect spring with constant sectional dimension *S*. Hence, taking a constant time unit Δt of the deformation of the spring on length z, the viscosity scaled with z as:

$$\eta^T \equiv k_o \cdot \frac{\Delta t}{S} \cdot z^T \tag{8}$$

The Eq.8 establishes a relation between the property of a perfect spring and the flow property of a fluid, but the properties of many fluids namely, the osmotic pressure and elastic properties, are reported as the properties of perfect gases with a correcting function or parameters which take into account the potential of interactions at work in the fluids. Therefore, the relative variation of the volume at constant external pressure P, (∂V/V), of fluids could be scaled with the relative variation of the volume of perfect gases by a factor *f* at a given temperature T. For a perfect gas, the relative variation of the volume is reported to be equal to the relative variation of the temperature (∂T/T). Hence, when the temperature varies, the volume of the fluid varies relatively as a factor of (∂T/T). Given that the fluid is modelled by a cylindrical spring with constant sectional area, the relative variation of its volume scaled with the relative variation of the temperature as:

$$\left(\frac{\partial z}{z}\right)_P = f^T \cdot \frac{\partial T}{T} \tag{9}$$

where in Eq.9 the factor $f = 1$ if the fluids were perfect gases. From Eqs.8 and 9 the relative variation of the viscosity (∂η/η), which is the derivation of the logarithm of the viscosity, Ln(η), scaled with (∂T/T) as (∂z/z).We define the derivation of the function $F(T)$ as $\partial F(T) = \partial\eta/\eta$, which gives the Eq.10

$$\frac{\partial F(T)}{\partial T} = f^{T} \cdot \frac{1}{T} \tag{10}$$

as the derivation of the logarithm of the temperature dependence of the viscosity η^T and that could be obtained experimentally. If the temperature is increased from T_o arbitrary initial condition of T, the viscosity η^T scaled as a factor of $Exp[F(T)-F(T_o)]$, which is the integral of the derivation of the function $F(T)$. The viscosity η^T could be scaled as $K_o \times Exp[F(T)]$ defining K_o (Eq.11) as the viscosity at the original conditions.

$$K_o = k_o \cdot z_o \cdot \frac{\Delta t}{S} \cdot e^{-F(T_o)} \tag{11}$$

However, the factor K_o is simplified by considering the viscosity at any reference temperatures T_1.

If the fluid is presented as a mass of particles or molecules without interactions between them, it is well described theoretically that the momentum of the particles, i.e., the fluids viscosity increases with the temperature. The water in the liquid state is a mass of water molecules interacting with each other. The evolution of the viscosity with the temperature of colloidal suspensions where the colloids interact is not easily predictable. This means that the temperature dependence of the interaction forces, which we refer to as dynamic, or virial mass is unknown. However, the viscosity of the suspension of free colloids increases with temperature. Therefore, the viscosity of the water should increase with the temperature when its molecules are able to move freely. This means that the interactions between the molecules are substantially weakened.

We hypothesise that the evolution of the viscosity of practically all liquid with the temperature on a large temperature interval may show where the contribution of the interactions between the liquid molecules are reduced. This should be evidenced if the viscosity is measured using a

force to measure the deformation for a given frequency. This means that, the pressure being constant, it should be possible to observe a decrease in the viscosity of the water but to a minimum with increasing the temperature to the critical temperature T_c where the water molecules mostly become free. Therefore, viscosity of a given fluid exists at two temperatures i) the temperature T_1 in the state of the fluid below T_c and ii) the T_2 in the state of the fluid above T_c. T_1 and T_2 are paired to the same viscosity. However, the model herein does not show precisely how the viscosity increases above the critical temperature T_c ~~(to the temperature T_2)~~. The theory of the viscosity of the perfect gas systems predicts that the viscosity of the systems as the average velocity of its particles is proportional to √T, which suggests that the thermal energy is exclusively converted to kinetic energy (Sutherland, 1893). We propose that the conditions $\eta(T_1) = \eta(T_2)$ are verified if $F(T_2) = F(T_1)$, therefore a second polynomial regression function is used for F(T) and expressed as:

$$F(T) - F(T_1) = B_2 \cdot (T - T_1) \cdot (T - T_2) \tag{12}$$

The minimum of Eq.12 may coincide with the minimum of the viscosity at the critical temperature T_c. B_2 reflects the thermal resistance of the fluid as a monophasic system. As such, B_2 is weak when it costs more energy to reach the viscosity of T_2. Therefore, B_2 somehow reflects the cost of energy reciprocally from expansion to evaporation of the liquid. The critical temperature which is $(T_1 + T_2)/2$ evolves as T_2. Thus, this model could use only one adjusting parameter i.e. B_2 if T_c was known or determined using other techniques. The viscosity of all the examined samples have been fitted using the function:

$$\eta^T = \eta^{T_1} \cdot Exp\left[B_2 \cdot (T - T_1) \cdot (T - T_2)\right] \tag{13}$$

For the present study, the reference T_1 = 20 °C and T_2 is determined by the fit function as well as B_2. The values of B_2 and T_c were examined as function of the polysaccharide concentration to show the influence of the polysaccharide on the solution resistance to thermal flow.

The experimental data of the concentration dependence of the viscosity for various temperatures were analysed using Huggins and Kraemer function to obtain the C* and the intrinsic viscosity [η] (Chronakis, Doublier & Piculell, 2000). The C* and [η] were evaluated as function of the temperature and the results used to discuss the thermal stability of the polysaccharide in solution.

3. Results and Discussion

3.1 Temperature dependence of the viscosity

The temperature dependence viscosity of the solvent (demineralized water with 200-ppm NaN_3) and kappa-carrageenan (kC) solutions from 0.12 g/L to 7.0 g/L were measured in the temperature intervals from 5 °C to 60 °C. The fit to Eq.13 data of demineralized water are shown in **Table 1** for the current viscosity data and the data of Korson et al. 1969 (Korson, Drost-Hansen & Millero, 1969). As aforementioned, it is imperative to note that the objective of determining the viscosity of demineralized water was not to report on the true value of the viscosity of water for the various temperatures but to use the appropriate viscosity of the solvent displayed by the instrument in our experimental conditions for the study.

Table 1*: The parameters of the fit to Eq.13 used to fit the temperature dependence of the water viscosity from the DHR3-Couette geometry and of the water viscosity data reported by Korson et al. 1969 (Korson, Drost-Hansen & Millero, 1969)*

Type of solvent (water)	Water + 200-ppm NaN_3	From the literature Korson et al. 1969
Instrument	DHR3 Rheometer with Couette geometry	Cannon-Ubbelohde Viscometer
η_0 (20 °C) reference	1.114 ± 0.030 mPa.s	1.002 mPa.s
T_1 (Liq.)	20.4 ± 0.5 °C	20.8 °C
T_2 (Gas)	180.0 ± 3.9 °C	256 °C
T_c	100.2 ± 1.7 °C	138.6 °C
B_2	1.57×10^{-4} °C^{-2}	1.01×10^{-4} °C^{-2}
R^2	0.995	0.999

The fit function is assumed to provide the appropriate solvent viscosity for the temperature given that beyond 50 °C, it was not possible to measure the viscosities of either the solvent or the samples at lower concentrations accurately. The concept on which the fit function is based on leads to the comparison of the critical temperature T_c with the water liquid-gas transitioning temperature. As we found a similar value, the coincidence is interesting for the acceptability of the model for calculating the viscosity for various temperatures from 0 °C to T_c. The coincidence could be fortuitous, because taking T_c from the viscosity data reported by Korson et al., 1969 (Korson, Drost-Hansen & Millero, 1969), one cannot tell exactly how the experimental set up influenced the accuracy of T_c.

Figure 2a shows the temperature ramp of the viscosity for the solvent and for various kC concentrations with the fit function, Eq.13, through the data. The mean square regression coefficient (R^2) for all of the samples and solvent examined lies between 0.988 and 1, the average of R^2 is 0.997 ± 0.003. The results show a strong correlation of the viscosity with the temperature, which characterizes the temperature dependence of the dynamic mass of the system. Given that the static mass (m) per unit of volume, which is explicitly the concentration, is constant, it is, therefore, the decrease of the dynamic mass (m_D) that causes the decrease of the viscosity when the temperature increases (**Figure 2a**). Thus, the increase of the temperature

leads the system constituents to behave more and more like an individual. The resistance of the constituents to behave like an individual characterizes somehow the affinity between the polymers and the polymers with the solvent molecules with which they form a monophasic system. This affinity within the solution is reflected by the fit parameters, namely the coefficient B_2 and T_c shown in **Figure 2b**.

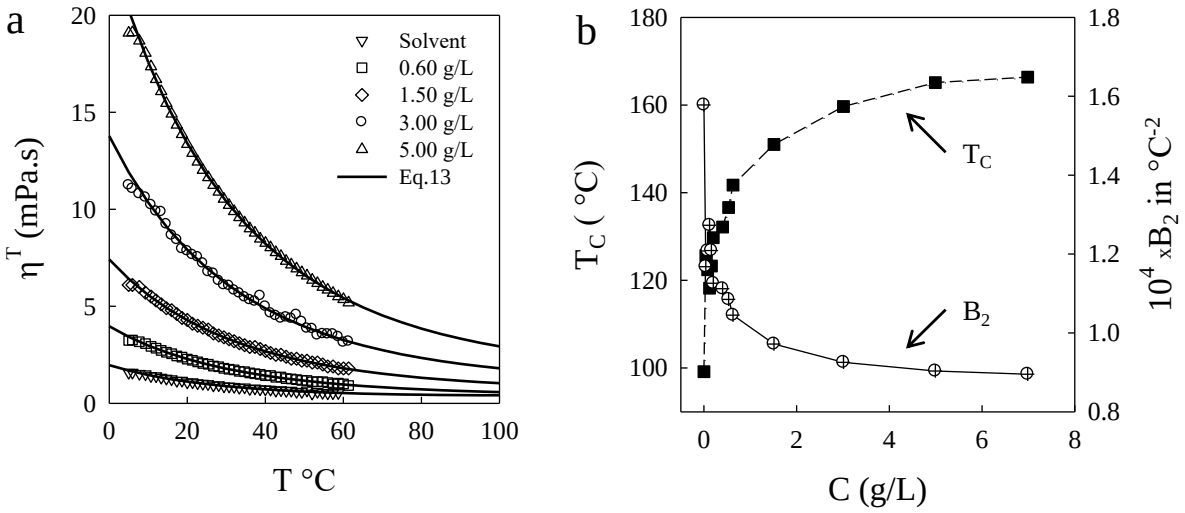

Figure 2: a) *Temperature dependence of the viscosity for various concentrations of kC solution. The full lines through the data are the fit function to Eq. 13.* ***b)*** *the fit parameters for B_2 and critical temperature, T_c, which is the temperature corresponding to the predicted minimum of the viscosity of the fluid where according to the model the liquid to gas transition are assumed to occur.*

The increase of the critical temperature or the diminution of the coefficient B_2 shows that the polysaccharide likes to dwell in the solvent (resistance to evaporation). As we look at the quantity $T_c \times B_2$, we found $1.5\times10^{-2} \pm 3.7\times10^{-4}$ /°C, the same value as that reported for the kC solution in presence of KCl salt by Elmarhoum and Ako 2021 (Elmarhoum & Ako, 2021). This value is almost constant on the interval of the concentrations studied in the present work, except for the solvent for which the value is 1.6×10^{-2} /°C. Thus, the quantity $T_c \times B_2$ depends on the presence of the polymer rather than the concentration. Therefore, the critical temperature

controls the temperature dependence of the viscosity by factor $T_c \times B_2$, which depends mainly on the system composition. Thus, the temperature dependence of the viscosity data could be fitted with the viscosity model using only one fit parameter because if T_c is known by other techniques, then B_2 remains the parameter to fit the temperature dependence of the viscosity data. The derivation of the polynomial function of Eq.10 could be expressed as:

$$\frac{1}{T} f^{T} = 2T_c B_2 \cdot \left(\frac{T}{T_c} - 1 \right) \tag{14}$$

with T between 0 °C and T_c (°C). The Eq.14 gives the quantity $T_c \times B_2$ as the absolute value of the limit of $(\partial\eta/\eta)$ when T → 0 °C. The negative value of the limit could be the result of the inter and intramolecular forces acting in the system to oppose its thermal deformation.

3.2 Concentration dependence of the viscosity

The viscosity values of the samples (η) were recorded at 20 °C, which is the temperature at which the viscosity of the reference was measured experimentally. The data are plotted versus the concentrations in log-log scale (**Figure 3**) for determining the relationship of the function between the viscosity and the concentration for this temperature as denoted in Eq.15

$$\eta - \eta_0 = \eta_0 \cdot a \cdot C^b \tag{15}$$

where η_0 is the solvent viscosity, a is an adjusting parameter and b is the scaling power. Eq.15 fairly fits well the viscosity data from the lower to the higher concentration (**Figure 3**, solid line). This shows that the specific viscosity $\eta_{sp} = (\eta - \eta_0)/\eta_0$, scales as a power law function of the concentration $\eta_{sp} \approx C^b$ as shown by the straight dash line in **Figure 3** which is in agreement with the scaling law theory for polymers in solution.

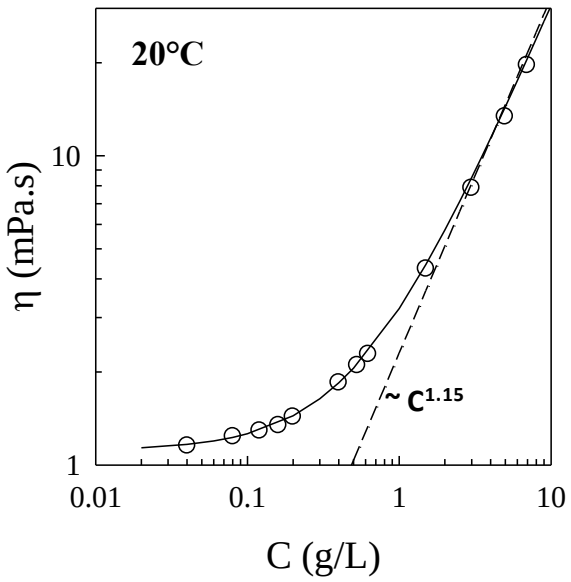

Figure 3*: Concentration dependence of the viscosity of kC solution for 20 °C. The solid and dash line represent the scaling law of the viscosity from the solvent viscosity and the viscosity increment with the concentration respectively. The dash line is comparable to the theoretical prediction of the viscosity for neutral flexible polymer in a good solvent ~$C^{1.3}$ at C < C*, i.e. the semi-dilute unentangled regime. The overlapping regime of the hydrodynamic volume for the kC is like unentangled regime for the neutral flexible polymer in good solvent because of likely repulsive interactions between the kC.*

The polymer in solution theory predicts a power law function of b ≈ 1.3 for a flexible polymer in a good solvent and ≈ 0.5 for polyelectrolyte in solution with no-salt for the concentrations in semi-dilute unentangled regime which concentration domain is identified here as dilute and semi-dilute regime (Colby, 2010). In the case of the present study, the value of b ≈ 1.15 is comparable to that of flexible polymer in good solvent weakly expanded by intramolecular repulsive forces.

The scaling power remains constant in the concentration intervals explored which means that the double logarithm plot of the η_{sp} versus concentration is not appropriate to determine the C*.

This seemingly is not what reflect the results reported by Croguennoc et al. 2000 and co-workers on the C* value using light scattering and rheometer methods (Croguennoc, Meunier, Durand & Nicolai, 2000). The authors determined the z-average radius of the coil, R_{gz} by light scattering measurement then used the Eq.16

$$C^* = \frac{3M_w}{4\pi N_A R_{gz}^3} \tag{16}$$

to obtain the C*, which gives C* = 0.45 g/L for the kC in 0.1 M NaCl solution. The C* from the viscosity measurement was estimated by using Huggins Eq.17 to derive the intrinsic viscosity $[\eta]_H$ by extrapolation to infinite dilution as the inverse of $[\eta]_H$, ($C^* \approx 1/[\eta]_H$).

$$\frac{\eta_{sp}}{C} = [\eta]_H + k_H [\eta]_H^2 C \qquad \text{Huggins} \tag{17}$$

which gives C* = 1.1 g/L for an intrinsic viscosity of 0.94 L/g for 4.3×10^5 g/mol in 0.1 M NaCl solution at 20 °C. Chronakis et al. 2000 (Chronakis, Doublier & Piculell, 2000) combined both Huggins Eq.17 and Kraemer Eq.18 to derive C* value by extrapolation to infinite dilution

$$\frac{Ln(\eta/\eta_0)}{C} = [\eta]_K + k_K [\eta]_K^2 C \qquad \text{Kraemer} \tag{18}$$

but the C* was not derived directly as the inverse of the intrinsic viscosity. It was determined as the transition point between two concentration regimes characterized by isolated coil kC in the dilute regime to coil overlap entangled semi-dilute regime as a change of the scaling power b. The authors found $C^* \approx 0.9$ g/L with an intrinsic viscosity of 2.34 L/g for 7×10^5 g/mol in 0.2 M NaI at 25 °C. The critical concentration determination from the viscosity measurement in log-log representation is very sensitive to the change of slope of the specific viscosity when turning the concentration from one regime to another. The difficulty of detecting the C* may be due to the weakness of the degree of the hindrance of the polymer motion due the presence

of others polymers when their hydrodynamic volume or the electrostatic potential shell length start overlapping. The repulsive interaction and the affinity of the polymer to the solvent may contribute to weakening of the hindrance effects around the C*. Therefore, changing the affinity between the solvent and the polysaccharide could result in better detection of the point at which the concentration regime changes. The concentration dependence of the viscosity of various temperatures including for 0 °C and 90 °C which were obtained from the fit (Eq.13), i.e. the temperature dependence of the viscosity for various concentrations are shown in **Figure 4**.

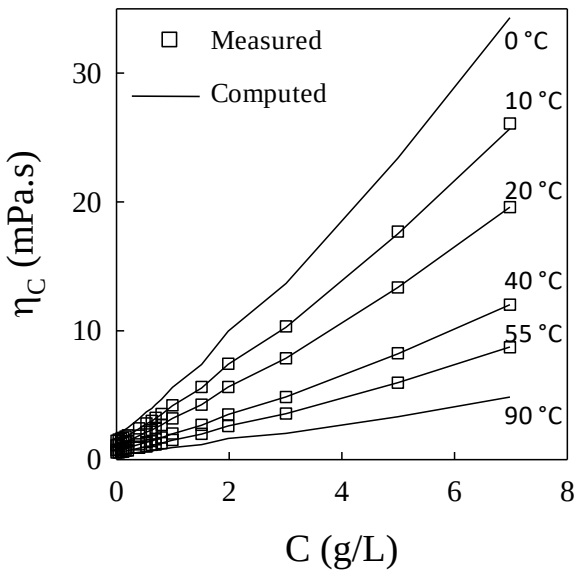

Figure 4*: Concentration dependence of the viscosity for various temperatures. The symbols are the measured data and the solid lines are the data obtained with Eq. 13.*

The specific viscosity is plotted as function of the concentration for various temperatures to identify the transition from dilute and semi-dilute regime for determining the C*. For a large range of temperature, from 0 °C to roughly 45 °C, the concentration where the slope changes was not clearly identified. Nevertheless, the slope changes more or less remarkably from temperature above 45 °C using the fit. The specific viscosity versus the concentration in double logarithm plot for 20 °C and 70 °C are shown in **Figure 5a** to illustrate the difficulty of identifying the C*. For 20 °C, no change of slope was observed. With the fit a change of the

slope at 70 °C was seen. The viscosity of the samples versus the concentration for 70 °C show a clear change of the scaling power slope from 1.1 to 1.6 characterizing the shift from semi-dilute to dilute regime respectively which is observed at a critical concentration of 0.54 g/L. Thus, the lower concentrations for determining the intrinsic viscosity are defined as concentration < 0.5 g/L. The intrinsic viscosities were determined by combined Huggins Eq.17, and Kraemer Eq.18, extrapolation to infinite dilution. The Huggins plot (H-plot) and Kraemer plot (K-plot) theoretically cross at [η] when C → 0. However, because of experimental imprecision the cross point does not occur exactly at the 0 axis of the concentration. Thus, we denote $[\eta]_H$ and $[\eta]_K$ the intrinsic viscosity from the H-plot and K-plot respectively. An illustration of the H-plot and K-plot for 20 °C and 40 °C are provided in **Figure 5b**. The plots are acceptably linear which give $[\eta]_H$ and $[\eta]_K$ respectively 1.23 L/g and 1.25 L/g for 20 °C, 1.10 L/g and 1.13 L/g for 40 °C. The intrinsic viscosity from both plots are similar. The concentration where the two plots cross is 0.02 g/L for 20 °C and 0.04 g/L for 40 °C. When the intrinsic viscosity ranges between 0.1 L/g and 2 L/g this characterizes an extended chain or very flexible chain rather than a compact coil as reported by Chronakis et al. 2000 (Chronakis, Doublier & Piculell, 2000).

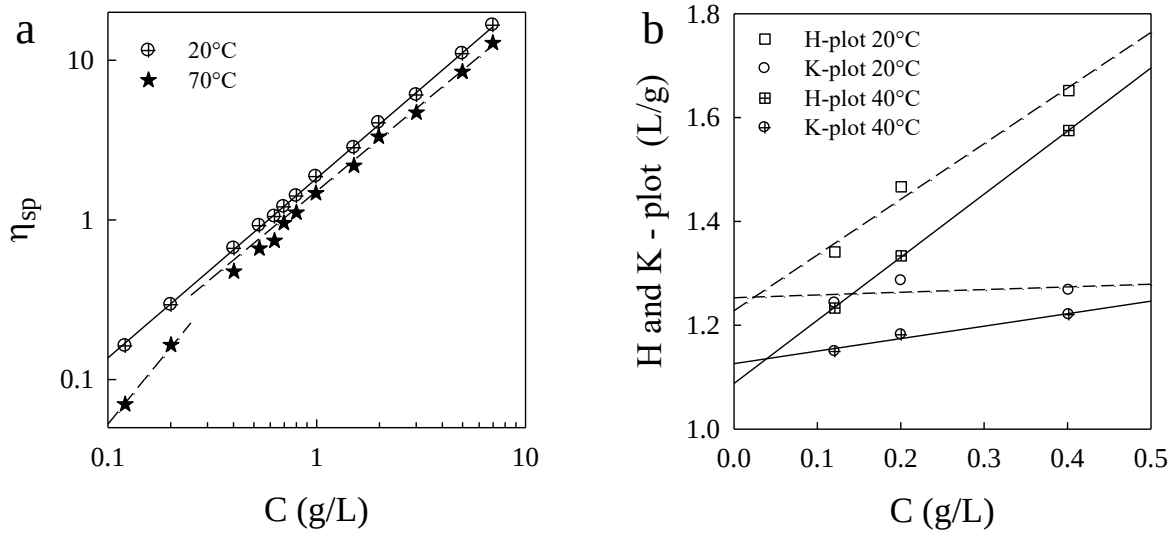

Figure 5: a) *Concentration dependence of the specific viscosity for 20 °C and 70 °C in double logarithmic plot. The data of 70 °C were predicted using Eq. 13. The solid and dash line represent the scaling law of the viscosity with the concentration as ~C^b where power-b is the slope of the lines.* *b) Is the Huggins Eq.17 and Kramer Eq.18 plot for the concentration lower than 0.5 g/L.*

Comparatively, the intrinsic viscosity of the current study is greater than what was reported by Croguennoc et al. 2000 for the same temperature but in the presence of 0.1 M NaCl (Croguennoc, Meunier, Durand & Nicolai, 2000). It is not surprising that we found a greater intrinsic viscosity because Slootmaker et al. 1988 have reported an increasing tendency of the intrinsic viscosity with decreasing the NaCl ionic strength for 3.3×10^5 g/mol kC (Slootmaekers, De Jonghe, Reynaers, Varkevisser & van Treslong, 1988). The intrinsic viscosity of kC was found to increase almost linearly as a function of the inverse root of the NaCl concentration (Slootmaekers, De Jonghe, Reynaers, Varkevisser & van Treslong, 1988). This gives roughly a corresponding presence of 10 mM NaCl for $[\eta] \approx 1.23$ L/g at 25 °C. Thus, there is a probability that traces of salt could still be in the kC solution after the dialysis step in the present study.

We found that when the Kraemer function (Eq.18) is plotted as function of Log(C) the plots clearly show the frontier between the concentration regimes for all the temperatures examined. We denoted this type of representation Kraemer-LogC or K-LogC. Therefore, we did the same with the Huggins function (Eq.17), Huggins-LogC or H-LogC. The H-LogC and K-LogC are shown in **Figure 6a** for 20 °C and in **Figure 6b** for 70 °C. For 20 °C the H-LogC does not show the existence of C* as it is clearly defined for the K-LogC. The K-LogC shows a C* for 20 °C at 0.45 g/L. In comparison with the result reported by Croguennoc et al. 2000, the C* is similar with the value that the authors found by light scattering technique, which corresponds to $R_{gz} \approx$ 66 nm using Eq.16 (Croguennoc, Meunier, Durand & Nicolai, 2000). However, for 70 °C both H-LogC and K-LogC showed the same position of C* at 0.55 g/L (**Figure 6b**).

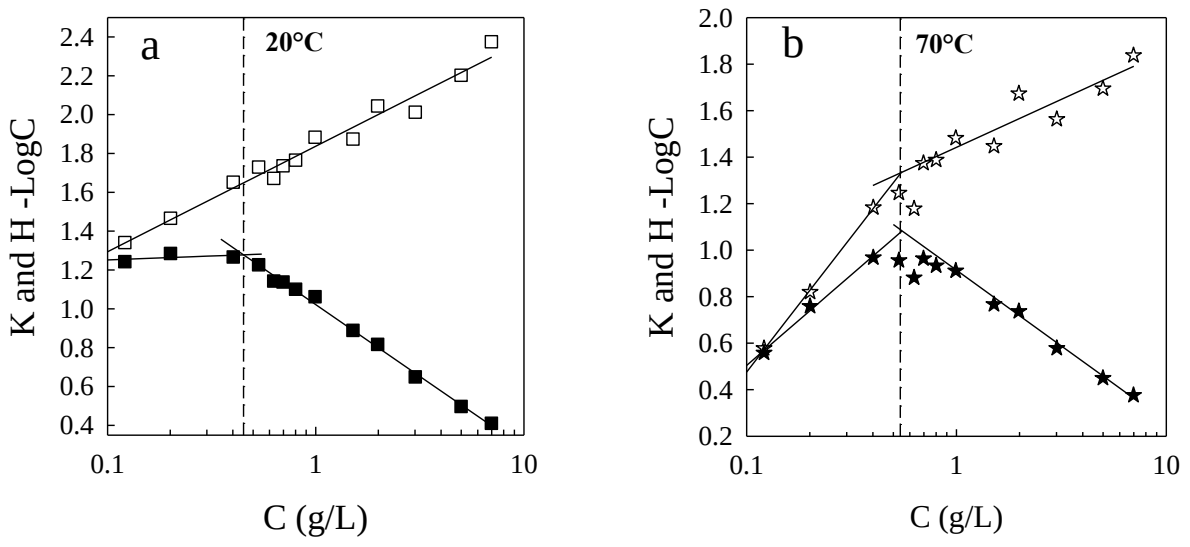

***Figure 6**: Concentration dependence of η_{sp}/C (Eq.17) open symbols and $Ln(\eta_r)/C$ (Eq. 18) full symbols in Lin-Log plot for a) 20 °C and b) 70 °C. The dash line indicates the C*.*

It results from the comparison of both methods for determining C* that Kraemer representation in Log(C) allows an accurate determination of C* of all the temperatures examined in this study. The following equations are therefore proposed for determining the C* but only Eq. 20 was used thereafter.

$$\frac{\eta_{sp}}{C} = A_H^* + A_H \cdot Ln(C) \tag{19}$$

$$\frac{Ln(\eta_C / \eta_0)}{C} = A_K^* + A_K \cdot Ln(C) \tag{20}$$

The coefficients of the Eqs.19 and 20 depend on the regime of concentration, but at C* both semi-dilute and dilute regime yield the same value.

The temperature dependence of the intrinsic viscosity, Huggins $[\eta]_H$ and Kraemer $[\eta]_K$, are shown in **Figure 7a**. Due to the considerable fluctuation of the measured viscosity of the solvent for T > 45 °C the intrinsic viscosity was not determined for the higher temperature. The model was used to extrapolate data to these temperatures (solid line). The intrinsic viscosity is maximum $[\eta] \approx 1.24$ L/g around 20 °C.

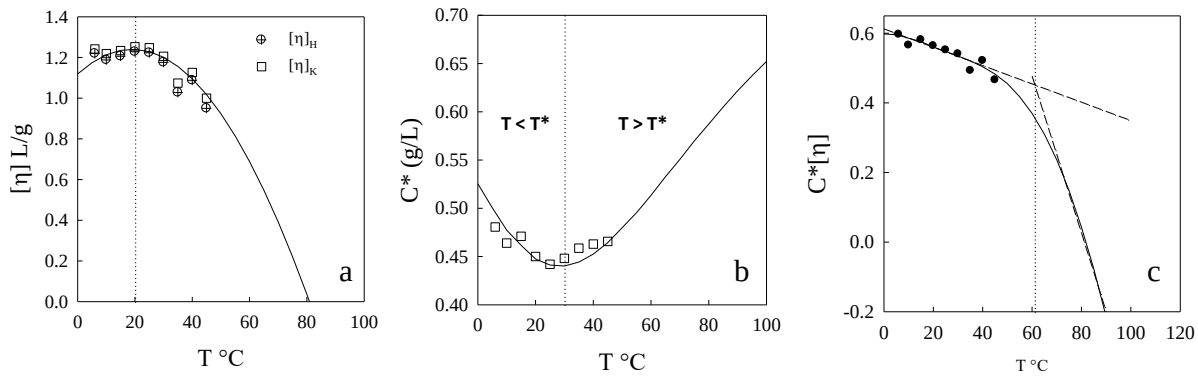

***Figure 7**: Temperature dependence of a) the intrinsic viscosity from both Huggins and Kraemer functions. The solid line represents the average results from the fit to Eq. 13 of the Huggins and Kraemer function, b) the critical concentration where the solid line represents the result from the fit to Eq.13 and T* is the temperature where the C* is lower. c) the dimensionless quantity C*[η] which could characterize the evolution of the amount of solvent molecules carried at C* by the polymer.*

The decrease of the intrinsic viscosity characterizes the diminution of the capacity for the polymer to increase the viscosity when its presence is increased in the solution. In the semi-dilute regime, this diminution of the thickening capacity result directly from the loss of affinity with the solvent. The fact that the affinity of the polysaccharide increases then decreases thereafter interrogates the complex relation between solvent-solvent molecular interactions and solvent-polysaccharide interactions. We hypothesize that when the temperature decreases below 20 °C the solvent-solvent molecular interactions prevail over the solvent-polysaccharide interactions. Above 20 °C, the heat weakens the physical bonds between the solvent molecules and the polysaccharide. Subsequent increase of heat increases the degree of liberty of the molecules to free motion. We propose that the thermal properties of the solvent are very crucial in understanding the intrinsic viscosity of the solutions. When approaching the liquid-solid transition of the solvent, the solvent-solvent molecular interactions, which characterize the m_D of the solvent, increases. The dynamic solvent molecules decreases accordingly and may behave differently than when the temperature approaches the liquid-gas transition. This thermal property of water may interfere with the polysaccharide capacity to carry the water molecules and to affect the intrinsic viscosity of the system when the temperature varies. For a system of a given quantity or mass of polysaccharides, the m_D increases with the amount of solvent carried. The viscosity of the system increases accordingly.

The temperature dependence of the critical concentration is shown in **Figure 7b**. At the critical concentration, the concentration of the global system is considered equal to the concentration of the volume occupied by a single polysaccharide blob. The solid line is data from the model. The lower C* corresponds to a higher hydrodynamic volume (Eq.16). The C* ≈ 0.44 g/L at T* ≈ 30 °C correspond to the maximum average of the chains hydrodynamic volume (**Figure 7b**). This means that the increase or decrease of the temperature from T* ≈ 30 °C leads to the shrinking of the polymer sizes. The intrinsic viscosity data shown in **Figure 7a**, suggest that

the temperature where the polymer expansion is higher is not necessarily equal to the temperature where the polysaccharides chains may bind the greatest amount of solvent molecules. However, the amplitude of variation of the C* with the temperature was weak to clearly show the minimum in the temperature range [10 °C - 45 °C] where the measurements were done. The minimum value of C* became evident after application of the model as the model gives the C* values for a larger range of temperature [0 °C - 100 °C]. For this polysaccharide system, the results from the model suggest that the capacity of the polysaccharide to increase the viscosity of the solution by its presence is higher at ≈ 20 °C, whereas the polymer expansion is higher at T* ≈ 30 °C which is a gap of 10 °C that could not be neglected. There is a possibility of the coincidence of both temperatures being fortuitous.

Slootmaekers et al., have reported the hydrodynamic volume as a characteristic parameter of hydrodynamic permeability of polymers (Slootmaekers, De Jonghe, Reynaers, Varkevisser & van Treslong, 1988). The hydrodynamic permeability of a polymer in solution could be understood as the permeability of a gel of this polymer at the critical concentration C* of the same hydrodynamic volume. The permeability of a gel characterizes the capacity of the gel to transmit fluid. Therefore, the higher the hydrodynamic volume which corresponds to lower C* of the polymer, the higher the permeability of the gel if the solvent in the polymer hydrodynamic volume is free. Given that a fraction of solvent in the hydrodynamic volume is linked to the polymers, the hydrodynamic permeability of the polymers would result from the intrinsic viscosity coefficient [η] too. Hence, the higher the amount of solvent that the polymer blobs could bind, the lower the amount of free solvent that could flow through them. Therefore, the polysaccharide's capacity to transmit fluid decreases with increasing both C* and [η]. The temperature dependence of the C* and [η] shows that when the systems' temperature decreases (cooling) the hydrodynamic volume and the intrinsic viscosity increase. From T* ≈ 30 °C, the hydrodynamic volume decreases but the intrinsic viscosity still increases until T ≈ 20 °C where

the intrinsic viscosity decreases. The two quantities are therefore independent. The intrinsic elastic property of the polysaccharide chains would be at work interfering with the dynamic induced by the solvent molecules adsorption to the expansion of the polymers (Draget et al., 2001). The enthalpy of adsorption and the elastic potential energy may control the hydrodynamic permeability of the system, which may evolve as a factor of the hydrodynamic volume per the intrinsic viscosity. For the system at C* the hydrodynamic volume per intrinsic viscosity gives an expression which is proportional to 1/C*[η]. Hence, the dimensionless quantity C*[η] gives the capacity to resist the flow of the solvent by the polymer at a given temperature. Therefore, when the quantity C*[η] increases the hydrodynamic permeability decreases (**Figure 7c**) which is characterized by the increase of the viscosity for the polymer in solution. C*[η] is connected with the Flory-Fox relationship Eq.21 (Morris, Cutler, Ross-Murphy, Rees & Price, 1981; Slootmaekers, De Jonghe, Reynaers, Varkevisser & van Treslong, 1988).

$$\Phi^* = \frac{4\pi}{3} N_A C^* [\eta] \tag{21}$$

For the present study, C*[η] increases linearly when the temperature decreases (cooling), which is indicated by the linear least squares fit (dash line) in **Figure 7c**. The slope of the linear correlation between C*[η] and T changes at the adsorption and desorption critical temperature $T_{ad} \approx 60$ °C from 2.6×10^{-3} /°C for T < 60 °C to 22.5×10^{-3} /°C for T > 60 °C. The fact that the hydrodynamic permeability of the polysaccharide increases sharply from $T_{ad} \approx 60$ °C when the temperature increases may energetically result from the dynamic of the adsorption and desorption reaction of the polysaccharide with the solvent molecule at this temperature. We propose this to be Gibbs energy of the reaction:

$$[kC] + x[H_2O] \Leftrightarrow [kC][H_2O]_x \qquad \text{R1}$$

$$\Delta G^o = -RT_{eq} Ln(K_{eq}) \qquad (22)$$

with K_{eq} the constant of the reaction equilibrium, may provide an explanation of the determination of the temperature T_{ad} from which the hydrodynamic permeability of the polysaccharide increases sharply. It was assumed that the polysaccharide hydration reaction equilibrium characterized by T_{eq} could determine the temperature T_{ad}, but this needs to be well documented.

The temperature dependence of the hydrodynamic permeability of the system is therefore determinant for understanding the water holding capacity of the polymers and syneresis property of the gels or bulk. Actually, the concentration of the gels or bulk is set constant while the hydrodynamic volume of the system constituents changes with the temperature. The change of constituent's hydrodynamic volume may lead to space vacancy (contraction) or overlapping hydrodynamic volume (swelling). If the initial concentration of the sample coincides with the minimum C* and if we assume that the sample gels at T* then our study demonstrates that for highly thermosensitive constituents at $T \neq T^*$, the bulk may evolve toward space vacancy which is characterized by solvent release (syneresis). Therefore, the concentration has to be increased to keep the solvent inside the gel as depicted in **Figure 8**. However, if the viscosity of the solvent at the temperature at which the sample is kept is predominant, i.e. for instance, when the temperature of the water approaches 0 °C, the solvent is capable of staying inside the gel because of low motion of the molecules.

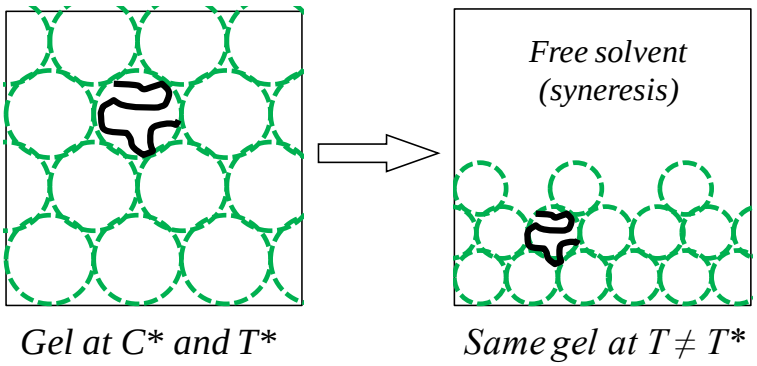

Figure 8*: Illustration of the syneresis from the situation where the gel is formed at C* and T*. T* is the temperature where the C* of the system is lower. The solution of the polymer at C* is pictured as a blobs of radius R_g in contact with each other to fill the space. The reduction of the size of the blobs due to conservation of the system at T ≠ T* leads to contraction of the blobs (Syneresis).*

4. Conclusion

The kC solution in the absence of additional salts shows a Newtonian flow behavior for the concentrations examined and a large temperature dependence of the critical concentration C* as the weight per volume of the blobs and of the intrinsic viscosity [η] of the volume of solvent carried by the blobs per their weight. The stability of these parameters characterise the thermodynamic stability of the polysaccharide in solution. The viscosity model applied in this study fits well the temperature dependence of the viscosity of the solvent and all the kC solutions with a $R^2 = 0.997 \pm 0.003$. According to the viscosity model the solution exhibits a minimum C* ≈ 0.44 g/L at temperature called lower critical concentration temperature and denoted LCCT which was found for the kC to be ≈ 30 °C and a maximum [η] ≈ 1.23 L/g or change of slope of the [η] at T ≈ 20 °C. The dimensionless quantity C*[η] was shown in this work to be the capacity of the polysaccharide to retain the solvent in solution. The C*[η] constantly decreases with the temperature from 0 °C to 45 °C following a slope of 2.6×10^{-3} /°C. The decrease became stronger from T ≈ 60 °C with a slope of 22.5×10^{-3} /°C. Cooling the kC

solution from higher temperature (≈ 100 °C) to the LCCT, the kC blobs expanded and carried more solvent molecules accordingly. From the LCCT to 20 °C, the kC blobs volume decreases but the blobs still carried more solvent molecules, leading to the assumption that the temperature dependence of the solvent density could be at work in the [η] value. From 20 °C to lower temperature (0 °C), the kC blobs constantly decrease and the amount of solvent molecules carried remained almost constant with a decreasing tendency. We hypothesise that pair interactions of solvent molecules may affect both the solvent density and the polymer-solvent interactions, and this plays a significant role in determining the intrinsic viscosity of hydrocolloid in solution. The water holding capacity as the hydrodynamic permeability of the polysaccharide is therefore determined fundamentally by both the pair interaction of solvent molecules with the polymers and the C* before gelation of the solution interferes with this.

5. Conflict of interest

The authors declare no conflicts of interest.

6. Acknowledgement

We thank Vincent VERDOOT for his technical assistance on the Rheometer Instruments. The authors thank Pr. Marguerite Rinaudo for providing us with the kappa-Carrageenan product. We thank Laurine Buon and Eric Bayma from Cermav for their kind assistance on the product composition. This work was financially supported by I-MEP2 PhD graduate school. The Laboratoire Rhéologie et Procédés (LRP) is part of the LabEx Tec 21 (Investissements d'Avenir - grant agreement n°ANR-11-LABX-0030) and of the PolyNat Carnot Institut Investissements d'Avenir - grant agreement n°ANR-11-CARN-030-01).

7. References

Ako, K. (2015). Influence of elasticity on the syneresis properties of kappa-carrageenan gels. *Carbohydrate Polymers, 115*, 408-414.

Berger, J., Reist, M., Mayer, J. M., Felt, O., & Gurny, R. (2004). Structure and interactions in chitosan hydrogels formed by complexation or aggregation for biomedical applications. *European Journal of Pharmaceutics and Biopharmaceutics, 57*, 35-52.

Boral, S., Saxena, A., & Bohidar, H. B. (2010). Syneresis in agar hydrogels. *International Journal of Biological Macromolecules, 46*, 232-236.

Brunchi, C.-E., Morariu, S., & Bercea, M. (2014). Intrinsic viscosity and conformational parameters of xanthan inaqueous solutions: Salt addition effect. *Colloids and Surfaces B, 122*, 512-519.

Campo, V. L., Kawano, D. F., da Silva Jr, D. B., & Carvalho, I. (2009). Carrageenans: Biological properties, chemical modifications and structural analysis - A review. *Carbohydrate Polymers, 77*, 167-180.

Chronakis, I. S., Doublier, J.-L., & Piculell, L. (2000). Viscoelastic properties for kappa- and iota-carrageenan in aqueous NaI from the liquid-like to the solid-like behaviour. *International Journal of Biological Macromolecules, 28*, 1-14.

Ciancia, M., Milas, M., & Rinaudo, M. (1997). On the specific role of coions and counterions on kappa-carrageenan conformation. *International Journal of Biological Macromolecules, 20*, 35-41.

Colby, R. H. (2010). Structure and linear viscoelasticity of flexible polymer solutions: comparison of polyelectrolyte and neutral polymer solutions. *Rheologica Acta, 49*, 425-442.

Croguennoc, P., Meunier, V., Durand, D., & Nicolai, T. (2000). Characterization of Semidilute k-Carrageenan Solutions. *Macromolecules, 33*, 7471-7474.

Divoux, T., Mao, B., & Snabre, P. (2015). Syneresis and delayed detachment in agar plates. *Soft Matter, 11*, 3677-3685.

Draget, K. I., Gaserod, O., Aune, I., Andersen, P. O., Storbakken, B., Stokke, B. T., & Smidsrod, O. (2001). Effects of molecular weight and elastic segment flexibility on syneresis in Ca-alginate gels. *Food Hydrocolloids, 15*, 485-490.

Drury, J. L., & Mooney, D. J. (2003). Hydrogels for tissue engineering: scaffold design variables and applications. *Biomaterials, 24*.

Einhorn-Stoll, U. (2018). Pectin-water interactions in foods - From powder to gel. *Food Hydrocolloids, 78*, 109-119.

Elmarhoum, S., & Ako, K. (2021). Lower critical concentration temperature as thermodynamic origin of syneresis: Case of kappa-carrageenan solution. *Carbohydrate Polymers, 267*.

Field, C. K., & Kerstein, M. D. (1994). Overview of Wound Healing in a Moist Environment. *The American Journal of Surgery, 167*.

Hoffman, A. S. (2012). Hydrogels for biomedical applications. *Advanced Drug Delivery Reviews, 64*, 18-23.

Kaur, L., Singh, N., & Sodhi, N. S. (2002). Some properties of potatoes and their starches II. Morphological, thermal and rheological properties of starches. *Food Chemistry, 79*, 183-192.

Klouda, L., & Mikos, A. G. (2008). Thermoresponsive hydrogels in biomedical applications. *European Journal of Pharmaceutics and Biopharmaceutics, 68*, 34-45.

Korson, L., Drost-Hansen, W., & Millero, F. J. (1969). Viscosity of Water at Various Temperatures. *The Journal of Physical Chemistry, 78*, 34-39.

Lai, V. M. F., Wong, P. A.-L., & Lii, C.-Y. (2000). Effects of Cation Properties on Sol-gel Transition and Gel Properties of k-carrageenan. *Journal of Food Science, 65*(8), 1332-1337.

Lee, M. H., Baek, M. H., Cha, D. S., Park, H. J., & Lim, S. T. (2002). Freeze-thaw stabilization of sweet potato starch gel by polysaccharide gums. *Food Hydrocolloids, 16*, 345-352.

Liu, Q., Subhash, G., & Moore, D. F. (2011). Loading velocity dependent permeability in agarose gel under compression. *Journal of the Mechanical Behavior of Biomedical Materials, 4*, 974-982.

Mao, R., Tang, J., & Swanson, B. G. (2001). Water holding capacity and microstructure of gellan gels. *Carbohydrate Polymers, 46*, 365-371.

Morris, E. R., Cutler, A. N., Ross-Murphy, S. B., Rees, D. A., & Price, J. (1981). Concentration and shear rate dependence of viscosity in random coil polysaccharide solutions. *Carbohydrate Polymers, 1*, 5-21.

Morris, V. J., & Chilvers, G. R. (1983). Rheological Studies of Specific Cation Forms of Kappa Carrageenan Gels *Carbohydrate Polymers, 3*, 129-141.

Munialo, C. D., Kontogiorgos, V., Euston, S. R., & Nyambayo, I. (2020). Rheological, tribological and sensory attributes of texture-modified foods for dysphagia patients and the elderly: A review. *International Journal of Food Science and Technology, 55*, 1862-1871.

Richardson, R. K., & Goycoolea, F. M. (1994). Rheological measurement of kappa-carrageenan during gelation. *Carbohydrate Polymers, 24*, 223-225.

Scherer, G. W. (1989). Mechanics of syneresis I. *Journal of Non-Crystalline Solids, 108*, 18-27.

Slootmaekers, D., De Jonghe, C., Reynaers, H., Varkevisser, F. A., & van Treslong, C. J. (1988). Static light scattering from κ-carrageenan solutions. *International Journal of Biological Macromolecules, 10*, 160-168.

Sutherland, W. (1893). The viscosity of gases and molecular force. *Philosophical Magazine Series 5, 36*, 507-531.

Takeshita, H., Kanaya, T., Nishida, K., & Kaji, K. (2001). Spinodal Decomposition and Syneresis of PVA Gel. *Macromolecules, 34*, 7894-7898.

Teko, E., Osseyi, E., Munialo, C. D., & Ako, K. (2021). The transitioning feature between uncooked and cooked cowpea seeds studied by the mechanical compression test. *Journal of Food Engineering, 292*, 110368-110376.

Vliet, T. v., Dijk, H. J. M. v., Zoon, P., & Walstra, P. (1991). Relation between syneresis and rheological properties of particle gels. *Colloid Polymer Science, 269*, 620-627.

Yousefi, A. R., & Ako, K. (2020). Controlling the rheological properties of wheat starch gels using Lepidium perfoliatum seed gum in steady and dynamic shear. *International Journal of Biological Macromolecules, 143*, 928-936.

Zhang, J., Ji, W., Liu, T., & Feng, C. (2016). Tuning Syneresis Properties of Kappa-Carrageenan Hydrogel by C2-Symmetric Benzene-Based Supramolecular Gelators. *Macromol. Chem. Phys., 217*, 1197-1204.